Band structure and phase stability of the copper oxides Cu_2O, CuO, and Cu_4O_3

Markus Heinemann,* Bianca Eifert,† and Christian Heiliger‡
I. Physikalisches Institut, Justus-Liebig-Universitaet, Heinrich-Buff-Ring 16, 35392 Giessen, Germany
(Received 14 January 2013; revised manuscript received 1 February 2013; published 7 March 2013)

The *p*-type semiconductor copper oxide has three distinct phases Cu_2O, CuO, and Cu_4O_3 with different morphologies and oxidation states of the copper ions. We investigate the structural stability and electronic band structure of all three copper oxide compounds using *ab initio* methods within the framework of density functional theory and consider different exchange correlation functionals. While the local density approximation (LDA) fails to describe the semiconducting states of CuO and Cu_4O_3, the LDA + U and HSE06 hybrid functional describe both compounds as indirect semiconductors. Using the HSE06 hybrid functional we calculate the electronic band structure in the full Brillouin zone for all three copper oxide compounds.

DOI: 10.1103/PhysRevB.87.115111 PACS number(s): 64.70.kg, 71.15.Mb, 71.20.Nr, 78.20.−e

I. INTRODUCTION

Prospective applications in the fields of optoelectronics and solar technology raise interest in the *p*-type semiconductor copper oxide and its three binary phases cuprous oxide (Cu_2O), cupric oxide (CuO), and paramelaconite (Cu_4O_3).[1,2] Consequently, there is a need for profound knowledge of the electronic and optical properties of these materials. For the first compound, Cu_2O, these features have been well studied in the past both experimentally[3–9] and theoretically.[10–20] As can be seen in Fig. 1(a), Cu_2O crystalizes in a cubic structure and each Cu^+ ion in the unit cell is coordinated by two oxygen ions. Cu_2O is naturally a *p*-type semiconductor and has a direct band gap of 2.17 eV and an optical gap of 2.62 eV.[2] While past research mainly focused on the excitonic features, recently cuprous oxide gained new interest as a sustainable and nontoxic absorber material for solar cells.[2]

Along with this new interest in the cubic phase of copper oxide, the optical and electronic properties of the remaining two structures CuO and Cu_4O_3 with respect to possible applications in the field of solar cell technology come into focus as well. CuO has a monoclinic crystal structure where Cu^{2+} ions are fourfold coordinated by oxygen. In the ground state, it has an antiferromagnetic order with a unit cell as demonstrated in Fig. 1(b). Furthermore, Fig. 1(c) illustrates the crystal structure of paramelaconite, which has a tetragonal symmetry. Here the crystal is built by twofold coordinated Cu^+ ions as in Cu_2O and fourfold coordinated Cu^{2+} ions as in CuO. Recently, Meyer *et al.*[2] demonstrated that all three copper oxide phases can be prepared by thin film deposition techniques. Their ellipsometric measurements of the dielectric function as well as their absorption measurements indicate that CuO and Cu_4O_3 are semiconductors with energy gaps roughly in the range of 1–2 eV. However, from the experimental side the exact size of the band gaps and the direct or indirect character of the band transition are still not conclusively determined.

From a theoretical point of view, the calculation of the electronic structure of these compounds is challenging. Traditional first-principles methods like the local density approximation (LDA) within density functional theory (DFT) fail to describe the materials as a semiconductor.[2,12] For monoclinic CuO, there exist only few full band structure calculations in literature that go beyond "standard" DFT: Wu *et al.*[16] use an LDA + U approach and find an indirect band gap of 1 eV, whereas Nolan and Elliot[15] see an indirect energy gap up to 2.1 eV depending on the U value using the same method. The strong dependence of these results on the U parameter as well as investigations of the electronic structure of Cu_2O which indicate that the LDA + U approach might not be sufficient to give a satisfying description of the electronic properties[21] clearly demand further investigation. Akin to the case of CuO, the electronic structure of Cu_4O_3 is also unclear. To our knowledge no band structure calculations that describe the semiconducting ground state of paramelaconite have been published up to now.

In this article we will present a comprehensive set of band structures from DFT hybrid functional calculations for the three copper oxide semiconductors Cu_2O, CuO, and Cu_4O_3. We further assess the structural properties and the phase stability of the three compounds and compare our results of the LDA + U and hybrid functional approach.

II. METHOD

All our calculations are performed using the VASP code[22–25] and the plane-wave based projector augmented wave (PAW) method.[26,27] The copper PAW potentials we use treat the Cu $3p^6$, $3d^{10}$, and $4s^1$ electrons as valence electrons. In the oxygen PAW potential, the O $2s^2$ and $2p^4$ electrons are chosen as valence states. For the exchange correlation functional we consider two functionals that go beyond the LDA to get a semiconducting description of all three copper oxide compounds. The first is the LDA + U approach where an additional potential is added to the LDA total energy expression that acts as an on-site intra-atomic interaction on the *d* states of copper. We choose the LDA + U method of Dudarev *et al.*,[28] which depends on the difference between two parameters U and J. In Ref. 29 Anisimov *et al.* propose a method which allows these parameters to be determined *ab initio*. For our calculations we adopt their values U = 7.5 eV and J = 0.98 eV which are calculated for a copper oxide system. The second exchange correlation functional we consider is the screened HSE06 hybrid functional[30–32] implemented in the VASP code.[33] Here a portion $\alpha = 25\%$ of exact nonlocal Hartree-Fock exchange is mixed into the exchange part of the PBE[34,35] total energy functional. The hybrid functional approach has proved very successful in

TABLE I. Cu_2O, CuO, and Cu_4O_3 equilibrium structural parameters, cell volume, and Cu–O bond lengths from LDA + U and hybrid functional calculations compared to experimental data.

	Parameter	LDA + U	HSE06	Experiment
Cu_2O	a (Å)	4.1656	4.2675	4.2696[2]
	Cu–O (Å)	1.80	1.85	1.85[2]
	Volume (Å^3)	72.28	77.72	77.83[2]
CuO	a (Å)	4.5882	4.5130	4.6837[37]
	b (Å)	3.3544	3.6121	3.4226[37]
	c (Å)	5.0354	5.1408	5.1288[37]
	β	99.39°	97.06°	99.54°[37]
	y	0.4186	0.4617	0.4184[37]
	Cu–O (Å)	1.92	1.94	1.96[37]
	Volume (Å^3)	76.81	83.49	81.08[37]
	Mag. moment	0.66 μ_B	0.54 μ_B	0.68 μ_B[38]
Cu_4O_3	a (Å)	5.6544	5.8392	5.837[39]
	c (Å)	9.7728	9.8966	9.932[39]
	z	0.1153	0.1142	0.117[39]
	Cu(I)–O(I) (Å)	1.81	1.85	1.87[39]
	Cu(II)–O(II) (Å)	1.87	1.91	1.92[39]
	Cu(II)–O(I) (Å)	1.93	1.98	1.97[39]
	Volume (Å^3)	312.46	337.44	338.38[39]
	Mag. moment	0.66 μ_B	0.71 μ_B	0.46–0.66 μ_B[40]

the description of the electronic structure of various oxide semiconductors, including Cu_2O, since it partially corrects systematic delocalization errors that are inherent in the LDA functional.[19,20,36]

For the calculations of the three copper oxide compounds we choose the plane-wave energy cutoff and the k-point sampling of the Brillouin zone such that total energy and structural parameters are well converged within less than 1%. For the LDA + U calculations we choose an $8 \times 8 \times 8$ k-point mesh and an energy cutoff of 800 eV for all three compounds. The computationally demanding hybrid calculations are performed using a cut-off energy ranging from 600 to 800 eV and a k-point sampling of $8 \times 8 \times 8$ for Cu_2O and $4 \times 4 \times 4$ for CuO and Cu_4O_3.

III. RESULTS

A. Structural relaxation

For each considered functional we perform a structural relaxation for all three copper oxide compounds. Cell shape and volume as well as ion positions are varied following a conjugate-gradient algorithm until the total energy of the system is minimized. The resulting equilibrium lattice parameters are listed in Table I and compared to experimental data.

The overall agreement between the structural parameters from both LDA + U and HSE06 calculations with experimental data is fairly good. Especially for the cubic Cu_2O and the tetragonal Cu_4O_3 the hybrid functional yields lattice parameters and bond lengths that are very close to the reference data. For the low-symmetry monoclinic structure of CuO the deviation of the calculated structural parameters from the experimental data is higher. Here the LDA + U approach seems to give more fitting results for the lattice parameters, but the Cu–O bond lengths and the cell volume are still better described by the hybrid functional.

CuO and Cu_4O_3 both have an antiferromagnetic ground state[38,40–42] that is crucial in the calculations to get a description of the electronic structure as a semiconductor. For CuO the antiferromagnetic unit cell has twice the size of the primitive unit cell of the crystal. In the case of Cu_4O_3 investigations suggest that the antiferromagnetic unit cell doubles the crystallographic unit cell in all three spacial directions.[42] Since the primitive unit cell already consists of 14 atoms, and to keep the computational effort of the hybrid-DFT calculations manageable, we choose the lowest energy state among the antiferromagnetic configurations that are realizable within the primitive cell. The magnetic moments are localized on the Cu^{2+} ions and their respective orientation is schematically depicted by the arrows in Fig. 1. The calculated values for these magnetic moments are also given in Table I.

B. Phase stability

Using the fully relaxed structures from the hybrid functional calculations, we investigate the thermodynamic stability of the three copper oxide phases in equilibrium with gas-phase O_2 at a specified pressure p_{O_2} and temperature T. Following the

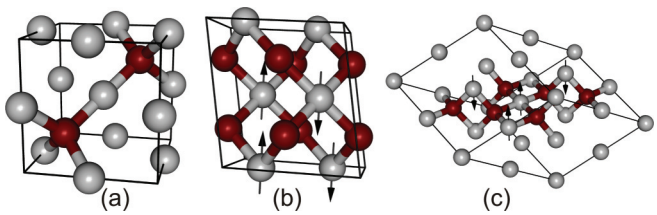

FIG. 1. (Color online) Cubic, monoclinic, and tetragonal crystal structure of the copper oxide compounds (a) Cu_2O, (b) CuO, and (c) Cu_4O_3. Gray: copper atoms, red: oxygen atoms. For the antiferromagnetic CuO and Cu_4O_3 the arrows on the copper ions indicate the orientation of local magnetic moments.

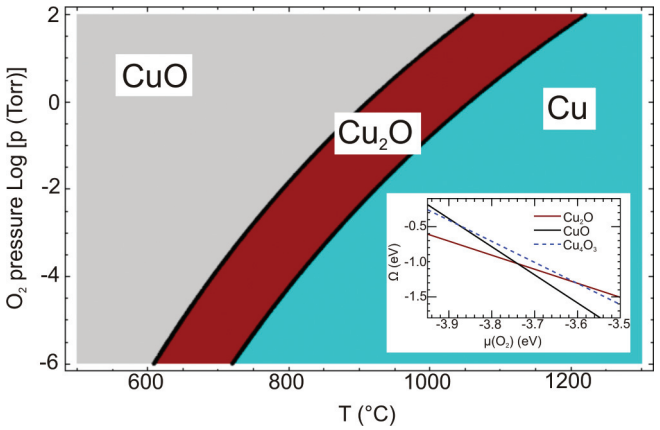

FIG. 2. (Color online) Calculated phase diagram of the copper oxide system using a DFT hybrid functional approach. Cu_4O_3 does not appear as a thermodynamically stable phase. The inlay shows the grand potential of CuO, Cu_2O, and Cu_4O_3 as a function of the oxygen chemical potential. Energies are normalized to cells containing eight copper atoms. The close position of the Cu_4O_3 grand potential at the phase transition between CuO and Cu_2O indicates a meta-stable state.

method described in Ref. 43, the phase with lowest grand potential determines the thermodynamically stable state at given p_{O_2} and T. Normalized to the same amount of copper atoms the grand potential of a phase i containing $N_{O,i}$ oxygen atoms can be calculated from the respective DFT-energy E_i according to[43] $\Omega_i(\mu_O) = E_i - \mu_O N_{O,i}$. We then correlate the oxygen chemical potential μ_O empirically to a pressure p_{O_2} and temperature T using the tabulated values given in Ref. 44. In this approach entropic contributions from lattice dynamics are neglected assuming that for crystalline structures their differences are small compared to the differences in internal energy from the electronic system.[43] Using a Debye model for the phonon density of states and the Debye temperatures $\theta = 184$ K for Cu_2O[45] and $\theta = 392$ K for CuO[46] we use the formalism of Ref. 47 to estimate the energy contributions from lattice vibrations to be in the order of 50 meV per Cu atom. Thus the accuracy of our phase transition temperatures lies within ± 30 K.

The calculated HSE phase diagram of the copper oxide system is shown in Fig. 2. The location of the phase transitions and the temperature dependence are in good agreement with the experimentally determined phase diagram in Ref. 48. The LDA + U approach, on the other hand, fails to describe these features correctly. Paramelaconite, Cu_4O_3, does not appear in the phase diagram in Fig. 2, i.e., from our calculations this phase is not a thermodynamically stable state. This result is also in agreement with the experimental phase diagram.[48] The inlay of Fig. 2 shows however, that at the phase transition between CuO and Cu_2O, the grand potential of paramelaconite lies energetically very close to those of CuO and Cu_2O. Including entropic effects thus might yield a stable phase for Cu_4O_3 as well. The fact that so far Cu_4O_3 has been prepared as thin films only also indicates that this compound is a meta-stable phase of copper oxide.

C. Electronic band structure

Following our investigation of the structural stability, we evaluate the electronic structure of all three copper oxide compounds from the LDA + U and hybrid functional approach. In both methods all three compounds are correctly described as semiconductors if one considers the antiferromagnetic ground states of CuO and Cu_4O_3 mentioned above. A simple LDA calculation, on the other hand, is not sufficient to give a description of a semiconductor for these two phases[2] and also fails to account for the antiferromagnetic state yielding zero local magnetic moments.

We give a comprehensive summary of the energy gaps of the three copper oxide phases we obtain from our various DFT calculations in comparison to other published calculations and experimental values in Table II. In addition, Fig. 3 illustrates the electronic band structures of the three compounds as calculated in the full Brillouin zone using the HSE06 hybrid functional. Figure 4 shows schematics of the Brillouin zones corresponding to the three crystal structures in Fig. 1 including

TABLE II. Energy gaps (in eV) of the copper oxide semiconductors Cu_2O, CuO, and Cu_4O_3 as obtained from our *ab initio* DFT calculations using different exchange correlation functionals in comparison to other calculations and experiments. For Cu_2O the direct band gap and the optical absorption threshold (i.e., the transition energy to the second conduction band) is given. For CuO and Cu_4O_3 we show the values of the indirect band gap as well as the smallest direct gap and its location. All our LDA + U calculations are performed using the values $U = 7.5$ eV and $J = 0.98$ eV obtained from Ref. 29.

		Present Work			Literature	
Compound	Gap	LDA	LDA + U	HSE	Theory	Experiment
Cu_2O	dir.	0.70	0.99	2.02	0.78 (OLCAO),[12] 1.77 (APW),[10] 0.54 (PW-LDA),[17] 0.60 (LAPW-LDA),[11] 0.63-0.94 (LDA + U),[20] 2.12 (HSE),[19] 0.79–2.77 (PBE0),[20] 1.97[17]–2.36[18] (scGW) 2.03 ($GW + V_d$)[49]	2.17[2]
	opt.	0.99	1.88	2.50	1.23 (PW-LDA),[17] 1.69 (LAPW-LDA),[11] 1.51 (G_0W_0@LDA),[17] 2.27[17]–2.81[18] (scGW) 2.7 ($GW + V_d$)[49]	2.62[2]
CuO	ind.	–	1.39	2.74	0.17–2.11 (DFT+U),[15,16,29] 1.3 (CI),[50] 1.0[51]–1.43[52] (LMTO-SIC) 1.19 ($GW + V_d$)[49]	1.4–1.7[2,6,53,54]
	dir.	–	1.91 (B)	3.26 (B)		
Cu_4O_3	ind.	–	1.27	2.54	–	1.34,[55] ∼1.5[2]
	dir.	–	1.47 (Γ)	2.71 (Γ)	–	

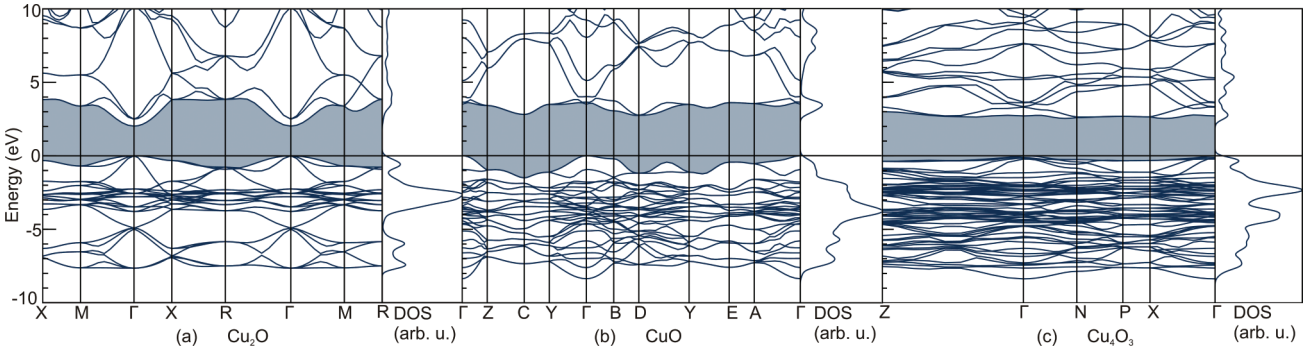

FIG. 3. (Color online) Electronic band structure and density of states of the three copper oxide compounds (a) Cu_2O, (b) CuO, and (c) Cu_4O_3 from hybrid functional DFT calculations. The corresponding Brillouin zones are given in Fig. 4. All three compounds are correctly described as a semiconductor. While Cu_2O has a direct band gap, for CuO and Cu_4O_3 an indirect energy gap appears. Values of the energy gaps are listed in Table II.

the location of the high symmetry k points along which the band structures are calculated.

In contrast to CuO and Cu_4O_3, the LDA already yields a semiconductor for Cu_2O. As can be seen from Table II, the resulting energy gap largely underestimates the actual band gap, which is a well known problem of this approximation. Since in Cu_2O the transition to the first conduction band is dipole forbidden, we also list the optical absorption threshold, i.e., the energy difference to the second conduction band at Γ in Table II. Using the LDA + U method does not improve the resulting band structure in a significant manner. Interestingly, varying the value of U has very little influence on the electronic structure. This can be explained by the complete occupation of the electron d shell in the Cu^+ ions in Cu_2O, which reduces the on-site correlation and hence the effectiveness of the LDA + U approach. Scanlon *et al.*[19] have shown that the hybrid functional HSE can successfully describe the electronic properties of cuprous oxide in the study of defect formation energies. By fine tuning the amount of the exact exchange contribution they were able to nearly reproduce the experimental band gap. In our calculation we use the "standard" value of $\alpha = 0.25$ and obtain energy gaps that deviate from the experimental gaps by less than 7%. Going beyond DFT, Bruneval *et al.*[17] and Kotani *et al.*[18] demonstrated that within the framework of many-body perturbation theory, a self-consistent approach to the GW approximation (scGW) is necessary to yield quasiparticle energies that are in very good agreement with experiment. The accuracy of these energy gaps is comparable to the HSE results at a much higher computational cost. Recently, Lany[49] proposed a GW scheme with an additional empirical on-site potential to adjust the copper d-orbitals and finds energy gaps for Cu_2O and CuO that are consistent with experiments.

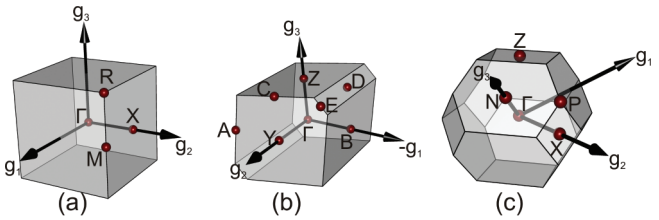

FIG. 4. (Color online) Brillouin zones with special high symmetry k points of cubic (a) Cu_2O, (b) monoclinic CuO, and (c) tetragonal Cu_4O_3.

Unlike in the case of Cu_2O, the use of the LDA + U strongly alters the outcome of the band structure calculation of CuO and Cu_4O_3, changing the electronic system from a metal (LDA) to a semiconductor with indirect band gap. In addition to the indirect energy gap we obtain in our calculations, we show the smallest direct gap and its respective location in the Brillouin zone in Table II. For both CuO and Cu_4O_3, our LDA + U band gaps are located closely to the experimental energy gaps reported in literature. Despite the good agreement with experimental energy gaps, the results of the LDA + U calculations are strongly dependent on the choice of the parameter U. Increasing U linearly shifts the conduction bands upwards and thus widens the energy gap. In contrast to recent absorption measurements on sputtered thin films[2] which suggest that Cu_4O_3 has a slightly larger energy gap than CuO, we see the opposite behavior throughout our calculations.

The hybrid functional band structures of CuO and Cu_4O_3 we plot in Fig. 3 show the same qualitative features as the electronic structure obtained from our LDA + U calculations. Quantitatively, the conduction bands are further shifted upwards, increasing the LDA + U energy gaps by about 1.3 eV. Hence, while for Cu_2O the HSE band gaps are in close distance to the experiment, the resulting band gaps for CuO and Cu_4O_3 overestimate the reported experimental values by approximately 1 eV. One has to keep in mind, however, that the experimental values are inconclusive for these two phases.

IV. CONCLUSION

In conclusion, we assess the structural stability and electronic band structure of the three copper oxide phases Cu_2O, CuO, and Cu_4O_3 from several approaches within density functional theory. The LDA + U and HSE06 hybrid functional both describe all three compounds as semiconductors, where Cu_2O has a direct band gap and CuO and Cu_4O_3 have indirect energy gaps. Our HSE06 energy gaps are in good agreement with experiment for Cu_2O, but there are discrepancies between experiment and theory for CuO and Cu_4O_3. We hope that our work will stimulate further experimental and theoretical investigations to clarify the electronic structure of these two compounds.

*markus.heinemann@physik.uni-giessen.de
†bianca.k.eifert@chemie.uni-giessen.de
‡christian.heiliger@physik.uni-giessen.de

[1]B. P. Rai, Sol. Cells **25**, 265 (1988).
[2]B. K. Meyer, A. Polity, D. Reppin, M. Becker, P. Hering, P. J. Klar, T. Sander, C. Reindl, J. Benz, M. Eickhoff, C. Heiliger, M. Heinemann, J. Bläsing, A. Krost, S. Shokovets, C. Müller, and C. Ronning, Phys. Status Solidi B **249**, 1487 (2012).
[3]P. W. Baumeister, Phys. Rev. **121**, 359 (1961).
[4]E. F. Gross and F. I. Kreihgol'd, J. Exp. Theor. Phys. Lett. (USSR) **7**, 218 (1968).
[5]S. P. Tandon and J. P. Gupta, Phys. Status Solidi B **37**, 43 (1970).
[6]J. Ghijsen, L. H. Tjeng, J. van Elp, H. Eskes, J. Westerink, G. A. Sawatzky, and M. T. Czyzyk, Phys. Rev. B **38**, 11322 (1988).
[7]A. Önsten, M. Månsson, T. Claesson, T. Muro, T. Matsushita, T. Nakamura, T. Kinoshita, U. O. Karlsson, and O. Tjernberg, Phys. Rev. B **76**, 115127 (2007).
[8]J. P. Hu, D. J. Payne, R. G. Egdell, P. A. Glans, T. Learmonth, K. E. Smith, J. Guo, and N. M. Harrison, Phys. Rev. B **77**, 155115 (2008).
[9]F. Haidu, M. Fronk, O. D. Gordan, C. Scarlat, G. Salvan, and D. R. T. Zahn, Phys. Rev. B **84**, 195203 (2011).
[10]J. P. Dahl and A. C. Switendick, J. Phys. Chem. Solids **27**, 931 (1966).
[11]P. Marksteiner, P. Blaha, and K. Schwarz, Z. Phys. B **64**, 119 (1986).
[12]W. Y. Ching, Y.-N. Xu, and K. W. Wong, Phys. Rev. B **40**, 7684 (1989).
[13]E. Ruiz, S. Alvarez, P. Alemany, and R. A. Evarestov, Phys. Rev. B **56**, 7189 (1997).
[14]R. Laskowski, P. Blaha, and K. Schwarz, Phys. Rev. B **67**, 075102 (2003).
[15]M. Nolan and S. D. Elliott, Phys. Chem. Chem. Phys. **8**, 5350 (2006).
[16]D. Wu, Q. Zhang, and M. Tao, Phys. Rev. B **73**, 235206 (2006).
[17]F. Bruneval, N. Vast, L. Reining, M. Izquierdo, F. Sirotti, and N. Barrett, Phys. Rev. Lett. **97**, 267601 (2006).
[18]T. Kotani, M. van Schilfgaarde, and S. V. Faleev, Phys. Rev. B **76**, 165106 (2007).
[19]D. O. Scanlon, B. J. Morgan, G. W. Watson, and A. Walsh, Phys. Rev. Lett. **103**, 096405 (2009).
[20]F. Tran and P. Blaha, Phys. Rev. B **83**, 235118 (2011).
[21]D. O. Scanlon, B. J. Morgan, and G. W. Watson, J. Chem. Phys. **131**, 124703 (2009).
[22]G. Kresse and J. Hafner, Phys. Rev. B **47**, 558 (1993).
[23]G. Kresse and J. Hafner, Phys. Rev. B **49**, 14251 (1994).
[24]G. Kresse and J. Furthmüller, Comp. Mat. Sci. **6**, 15 (1996).
[25]G. Kresse and J. Furthmüller, Phys. Rev. B **54**, 11169 (1996).
[26]P. E. Blöchl, Phys. Rev. B **50**, 17953 (1994).
[27]G. Kresse and D. Joubert, Phys. Rev. B **59**, 1758 (1999).
[28]S. L. Dudarev, G. A. Botton, S. Y. Savrasov, C. J. Humphreys, and A. P. Sutton, Phys. Rev. B **57**, 1505 (1998).
[29]V. I. Anisimov, J. Zaanen, and O. K. Andersen, Phys. Rev. B **44**, 943 (1991).
[30]J. Heyd, G. E. Scuseria, and M. Ernzerhof, J. Chem. Phys. **118**, 8207 (2003).
[31]J. Heyd and G. E. Scuseria, J. Chem. Phys. **121**, 1187 (2004).
[32]J. Heyd, G. E. Scuseria, and M. Ernzerhof, J. Chem. Phys. **124**, 219906 (2006).
[33]J. Paier, R. Hirschl, M. Marsman, and G. Kresse, J. Chem. Phys. **122**, 234102 (2005).
[34]J. P. Perdew, K. Burke, and M. Ernzerhof, Phys. Rev. Lett. **77**, 3865 (1996).
[35]J. P. Perdew, K. Burke, and M. Ernzerhof, Phys. Rev. Lett. **78**, 1396 (1997).
[36]P. Mori-Sánchez, A. J. Cohen, and W. Yang, Phys. Rev. Lett. **100**, 146401 (2008).
[37]S. Åsbrink and L.-J. Norrby, Acta Crystallogr. Sect. B **26**, 8 (1970).
[38]B. X. Yang, J. M. Tranquada, and G. Shirane, Phys. Rev. B **38**, 174 (1988).
[39]M. O'Keeffe and J.-O. Bovin, Am. Mineral. **63**, 180 (1978).
[40]L. Pinsard-Gaudart, J. Rodriguez-Carvajal, A. Gukasov, and P. Monod, Phys. Rev. B **69**, 104408 (2004).
[41]H.-J. Koo and M.-H. Whangbo, Inorg. Chem. **42**, 1187 (2003).
[42]M.-H. Whangbo and H.-J. Koo, Inorg. Chem. **41**, 3570 (2002).
[43]D. S. Sholl and J. A. Steckel, *Density Functional Theory* (Wiley, New York, 2009).
[44]NIST-JANAF thermochemical tables, http://kinetics.nist.gov/janaf/html/O-029.html.
[45]A. Kirfel and K. Eichhorn, Acta Crystallogr. Sect. A **46**, 271 (1990).
[46]A. Junod, D. Eckert, G. Triscone, J. Müller, and W. Reichardt, J. Phys. Cond. Matt. **1**, 8021 (1989).
[47]K. Reuter and M. Scheffler, Phys. Rev. B **65**, 035406 (2001).
[48]R. Schmidt-Whitley, M. Martinez-Clemente, and A. Revcolevschi, J. Cryst. Growth **23**, 113 (1974).
[49]S. Lany, Phys. Rev. B **87**, 085112 (2013).
[50]Z.-x. Shen, J. W. Allen, J. J. Yeh, J. S. Kang, W. Ellis, W. Spicer, I. Lindau, M. B. Maple, Y. D. Dalichaouch, M. S. Torikachvili, J. Z. Sun, and T. H. Geballe, Phys. Rev. B **36**, 8414 (1987).
[51]A. Svane and O. Gunnarsson, Phys. Rev. Lett. **65**, 1148 (1990).
[52]Z. Szotek, W. M. Temmerman, and H. Winter, Phys. Rev. B **47**, 4029 (1993).
[53]F. P. Koffyberg and F. A. Benko, J. Apl. Phys. **53**, 1173 (1982).
[54]F. Marabelli, G. B. Parravicini, and F. Salghetti-Drioli, Phys. Rev. B **52**, 1433 (1995).
[55]J. F. Pierson, A. Thobor-Keck, and A. Billard, Appl. Surf. Sci. **210**, 359 (2003).